Journal of Electrical Engineering, Vol. 76, No. 2, 2025, pp. 124-133

Selected harmonic minimization in 3-phase 11-level switch-switch multilevel inverter using artificial gorilla troops optimization algorithm

Yee Wei Sea[1], Wei Tik Chew[1], Siok Lan Ong[2], Quan Ming Wong[1,3], Ahmad Firdaus Ahmad Zaidi[1], Jenn Hwai Leong[1*]

A key challenge in designing 3-phase multilevel inverters (MLIs) is determining the switching angles that produce a low THD output voltage waveform. This work proposes an AGTO-SHMPWM technique for determining the switching angles, aiming to minimize low-order harmonics while achieving the desired fundamental harmonic. MATLAB analysis shows that the AGTO method achieves significantly lower objective function (*OF*) values, as low as 10^{-32}, compared to the GA and GOA methods. Cumulative distribution function analysis reveals that the AGTO method has a 38% probability of achieving an $OF \leq 10^{-30}$, while the GA and GOA methods have a 0% probability. These results demonstrate that the AGTO method is more capable of thoroughly exploring the optimization solution space. PSIM simulation confirms that the switching angles computed using the AGTO method, when applied to a 3-phase 11-level switch-switch MLI (S2MLI), can produce sinusoidal-like staircase voltage waveforms with minimized V_5, V_7, V_{11} and V_{13} harmonics while achieving the desired fundamental voltage. The phase and line-to-line voltage THDs, when the S2MLI is operated at M_{idx} of 0.80, are 7.93% and 5.55%, respectively, which are consistent with those predicted by MATLAB analysis.

Keywords: multilevel inverter, switching-angle computation, selective harmonic minimization, pulse-width modulation, artificial gorilla troops optimization, grasshopper optimization algorithm and genetic algorithm

1 Introduction

Multilevel inverter (MLI) is a DC/AC converter capable of producing a low total harmonic distortion (THD) output voltage waveform [1]. Three-phase (3-ph) MLIs have been employed in medium-to-high power applications owing to their advantageous characteristics, such as the feasibility of being constructed using power switches with lower voltage rating, lower *dv/dt* and lower electromagnetic interference [2-4]. Numerous topologies of MLI have been introduced in the literature, including switch-switch MLIs (S2MLI), cascaded H-bridge MLIs (CHBMLI), flying capacitor MLIs and diode-clamped MLIs [5-8]. Among these MLI topologies, the S2MLI stands out for requiring the fewest power switches, making it a more favorable choice for 3-ph systems.

Pulse-width modulation (PWM) techniques are common techniques employed for controlling the MLI [9]. Various PWM techniques have been developed and introduced, such as space vector PWM (SVPWM) techniques and sinusoidal PWM (SPWM) [10-11]. However, both SPWM and SVPWM techniques operate the power switches at high frequencies, resulting in significant switching losses. The switching losses can be reduced by utilizing a low switching frequency PWM technique known as selective harmonic minimization pulse-width modulation (SHMPWM) technique [12-13]. This technique aims to minimize the selected low-order harmonics, while controlling the fundamental harmonic at a desired value. To achieve this, solving a set of harmonic equations is required to obtain the switching angles for the MLI. In the literature, these equations have been solved using Newton-Raphson (NR) method [14-15]. However, this method heavily relies on a good initial guess of the switching angles [16]. Guessing the switching angles can be time-consuming, as it involves extensive trial and error and requires significant guessing experience.

Alternatively, these harmonic equations can be solved by converting them into an objective function (*OF*), which is subsequently minimized using the soft-computing (SC) method [17-18]. Examples of SC methods include the grasshopper optimization algorithm (GOA) and genetic algorithm (GA) [19-20]. These methods can solve the equations without heavily depending on the good initial guesses of the switching angles. However, they do not always guarantee effective minimization of the *OF*. Recently, a nature-inspired SC method called Artificial Gorilla Troops Optimization (AGTO) was introduced [21]. The AGTO has been

[1] Faculty of Electrical Engineering & Technology, Universiti Malaysia Perlis, Malaysia
[2] Faculty of Electronic Engineering & Technology, Universiti Malaysia Perlis, Malaysia
[3] Keysight Technologies, 11920, Penang, Malaysia
[*] corresponding author: jhleong@unimap.edu.my

https://doi.org/10.2478/jee-2025-0013, Print (till 2015) ISSN 1335-3632, On-line ISSN 1339-309X

successfully utilized in various engineering problems, such as optimizing power system stabilizers parameters, maximum power harvesting for thermoelectric generation system and reducing energy usage in wireless sensor networks [22-24].

To the best of the authors' knowledge, the feasibility of the AGTO method in solving the SHMPWM problem for a 3-ph MLI has not been previously reported. To bridge this gap, this work proposes an AGTO-SHMPWM technique for a 3-ph 11-level (11L) S2MLI. The contributions of this work are as follows:

(a) Proposing the AGTO-SHMPWM technique for a 3-ph 11L S2MLI.

(b) Comparison of the performance of the AGTO-SHMPWM technique to that of GA- and GOA-SHMPWM techniques.

(c) Evaluation of the proposed technique performance under resistive and inductive load conditions.

(d) Evaluation of the proposed technique performance under changing frequency conditions.

2 Three-phase eleven-level switch-switch MLI

Figure 1 illustrates the schematic diagram of a 3-ph 11L S2MLI. Each phase of the S2MLI comprises five DC voltage sources, labelled as V_{S1} to V_{S5}, along with 14 power switches, labelled as Q_{a01} to Q_{a14}. It is worth to highlight that the 3-ph 11L S2MLI requires less power switches than the CHBMLI. By way of example, the S2MLI requires only 42 power switches to construct the 3-ph 11L configuration, while the CHBMLI requires 60 power switches for the same configuration. Note that in this work, all five DC voltage sources are assumed to be equal in magnitude ($V_{S1} = V_{S2} = V_{S3} = V_{S4} = V_{S5} = V_S$). Figure 2 shows a typical output phase voltage waveform of the 3-ph 11L S2MLI and the five switching angles denoted as α_1, α_2, α_3, α_4 and α_5. These switching angles must be computed properly in order to produce a low THD output voltage waveform. Table 1 presents the derivation of the output phase voltage levels for phase A of 3-ph 11L S2MLI. Note that the OFF state of the power switches is represented by "0", while the ON state is represented by "1". The resultant waveform consists of eleven distinct voltage levels. Among them, one is zero voltage level, five are positive voltage levels ($+V_S$, $+2V_S$, $+3V_S$, $+4V_S$ and $+5V_S$) and five are negative voltage levels ($-V_S$, $-2V_S$, $-3V_S$, $-4V_S$ and $-5V_S$).

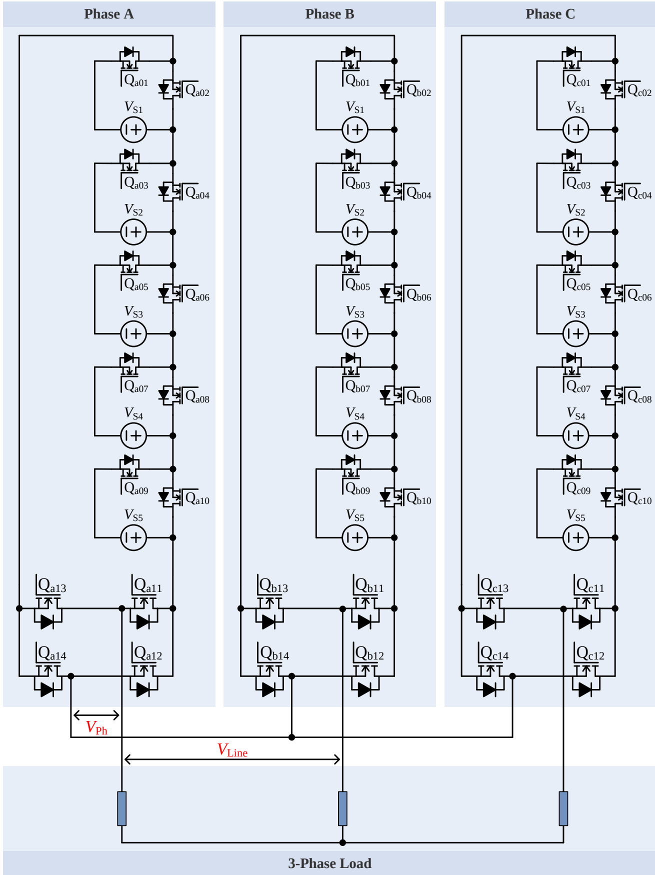

Fig. 1. Schematic diagram of 3-ph 11L S2MLI

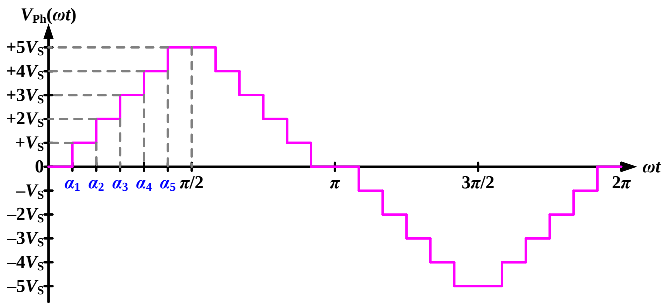

Fig. 2. V_{Ph} waveform of phase A 11L S2MLI

Table 1. Derivation of output phase voltage levels for phase A of 3-ph 11L S2MLI

Power switches	Output Phase Voltage Levels										
	0	$+V_S$	$+2V_S$	$+3V_S$	$+4V_S$	$+5V_S$	$-V_S$	$-2V_S$	$-3V_S$	$-4V_S$	$-5V_S$
Q_{a01}	0	1	1	1	1	1	1	1	1	1	1
Q_{a02}	1	0	0	0	0	0	0	0	0	0	0
Q_{a03}	0	0	1	1	1	1	0	1	1	1	1
Q_{a04}	1	1	0	0	0	0	1	0	0	0	0
Q_{a05}	0	0	0	1	1	1	0	0	1	1	1
Q_{a06}	1	1	1	0	0	0	1	1	0	0	0
Q_{a07}	0	0	0	0	1	1	0	0	0	1	1
Q_{a08}	1	1	1	1	0	0	1	1	1	0	0
Q_{a09}	0	0	0	0	0	1	0	0	0	0	1
Q_{a10}	1	1	1	1	1	0	1	1	1	1	0
Q_{a11}	1	1	1	1	1	1	0	0	0	0	0
Q_{a12}	1	0	0	0	0	0	1	1	1	1	1
Q_{a13}	0	0	0	0	0	0	1	1	1	1	1
Q_{a14}	0	1	1	1	1	1	0	0	0	0	0
Note: "0" representing OFF state and "1" representing ON state											

3 Artificial gorilla troops optimization-based SHMPWM technique

By applying the Fourier series, the output phase voltage waveform of the 3-ph 11L S2MLI shown in Fig. 2 can be mathematically represented as follows

$$V_{\mathrm{Ph}}(\omega t) = \sum_{n=1}^{\infty} \frac{4V_{\mathrm{S}}}{n\pi} \sum_{k=1}^{5} \cos(n\alpha_k)\ \sin(n\omega t) \tag{1}$$

where V_S is the magnitude of DC voltage source, n is an integer representing the odd n-th harmonic order, k is an integer, α_k is the k-th switching angle, ω is the angular frequency and t is time. Note that the switching angles applied to the S2MLI must meet the condition $0 \le \alpha_1 \le \alpha_2 \le \alpha_3 \le \alpha_4 \le \alpha_5 \le \pi/2$. The n-th harmonic amplitude in the V_{Ph}, as given in (1), is given as follows

$$V_n = \frac{4V_{\mathrm{S}}}{n\pi} \sum_{k=1}^{5} \cos(n\alpha_k) \tag{2}$$

In the SHMPWM technique, the fundamental harmonic is to be maintained at a desired value, while selected low-order harmonics are to be minimized. For the case of 3-ph 11L S2MLI, four undesired harmonics, i.e. 5-th, 7-th, 11-th and 13-th harmonics, are targeted for minimization. The equations for the fundamental and the four undesired low-order harmonics, derived from (2), are expressed as follows:

$$\begin{aligned} V_1 &= \frac{4V_{\mathrm{S}}}{\pi} \sum_{k=1}^{5} \cos(\alpha_k) \\ V_5 &= \frac{4V_{\mathrm{S}}}{5\pi} \sum_{k=1}^{5} \cos(5\alpha_k) \\ V_7 &= \frac{4V_{\mathrm{S}}}{7\pi} \sum_{k=1}^{5} \cos(7\alpha_k) \\ V_{11} &= \frac{4V_{\mathrm{S}}}{11\pi} \sum_{k=1}^{5} \cos(11\alpha_k) \\ V_{13} &= \frac{4V_{\mathrm{S}}}{13\pi} \sum_{k=1}^{5} \cos(13\alpha_k) \end{aligned} \tag{3}$$

where V_1 is the fundamental harmonic, while V_5, V_7, V_{11} and V_{13} are the 5-th, 7-th, 11-th and 13-th harmonics, respectively. Due to the 3-ph configuration of the MLI, the triplen-odd harmonics, such as V_3, V_9, V_{15}…, are not considered as they do not appear in the line-to-line voltage [25]. The modulation index (M_{idx}) of the 3-ph 11L S2MLI can be expressed as follows:

$$M_{\mathrm{idx}} = \frac{\pi V_1}{20V_{\mathrm{S}}} \tag{4}$$

where $0 < M_{idx} \le 1$. As previously mentioned, (3) can be solved using the NR method. Solving (3) simultaneously with NR method, however, is relatively time-consuming due to the need to guess good initial switching angles. Additionally, poor initial guesses may lead to convergence failure, making it unable to compute switching angles for a wide range of M_{idx}. To address these issues, the equations in (3) are converted into an *OF*, as presented in (5), and solved using SC methods. The *OF* is expressed as follows

$$\begin{aligned} OF = {} & \left(100\frac{V_{\mathrm{d}} - V_1}{V_{\mathrm{d}}}\right)^4 + \frac{1}{5}\left(50\frac{V_5}{V_1}\right)^2 + \frac{1}{7}\left(50\frac{V_7}{V_1}\right)^2 \\ & + \frac{1}{11}\left(50\frac{V_{11}}{V_1}\right)^2 + \frac{1}{13}\left(50\frac{V_{13}}{V_1}\right)^2 \end{aligned} \tag{5}$$

where V_d is the desired V_1. The first term of the *OF* focuses on evaluating how close the fundamental voltage is to the desired value, while the second to fifth terms focus on the minimization of the undesired V_5, V_7, V_{11} and V_{13} harmonics. As previously mentioned, the AGTO method [21] is employed and adapted to solve the SHMPWM problem in this work. The AGTO mimics the social behaviors of gorilla troops in nature. It involves two optimization phases, which are exploration and exploitation phases in the search for the best solutions.

In the exploration phase of the AGTO algorithm, three equations shown in (6) are used to mimic the behavior of the gorilla troop migrating to an unknown location, joining another gorilla troop or moving towards a known location. A parameter p, representing the probability of selecting the migration mechanism to an unknown space, is initialized at the beginning of the optimization process with a value between 0 and 1. The first equation in (6) is applied when $r_4 < p$. If $r_4 \geq 0.5$, the second equation in (6), which represents the behavior of the gorilla troop joining another troop, is selected. Otherwise, if $p \leq r_4 < 0.5$, the third equation in (6), which represents the behavior of the gorilla troop migrating to a known location, is chosen.

$$GY(j+1) = \begin{cases} r_1(Y_{\mathrm{UB}} - Y_{\mathrm{LB}}) + Y_{\mathrm{LB}} & r_4 < p \\ (r_2 - C)\cdot Y_r(j) + C\cdot l\cdot Z\cdot Y(j) & r_4 \geq 0.5 \\ Y(j) - (C^2 l^2 + C\cdot l\cdot r_3)\big(Y(j) - GY_r(j)\big) & p \leq r_4 < 0.5 \end{cases} \quad (6)$$

where j is the j-th iteration, $GY(j+1)$ represents the new position vector of gorilla in the $(j+1)$ iteration, while Y_{UB} and Y_{LB} are the upper and lower boundaries of the variables, respectively. $Y(j)$ is the current position vector of gorilla, and $Y_r(j)$ and $GY_r(j)$ are the position vectors of a gorilla chosen randomly from the entire population. Z is a randomly selected value between $[-C, C]$, l is a randomly selected value within the range of –1 and 1, and r_1, r_2, r_3 and r_4 are randomly selected values between 0 and 1 during every iteration. The value C is given by

$$C = (\cos(2r_5) + 1)\left(1 - \frac{j}{j_{\max}}\right) \quad (7)$$

where r_5 is a value selected randomly between 0 and 1 during every iteration and $j_{\max}$ is the maximum number of iterations. The OF of each GY solution is evaluated upon completing the exploration phase. If the OF of $GY(j)$ is lower than the OF of $Y(j)$, the $GY(j)$ solution will replace the $Y(j)$ solution. At the end of this phase, the GY solution with the lowest OF is referred to as the silverback (Y_{sb}).

In the exploitation phase of the AGTO algorithm, two mathematical equations, which are given by (8) and (9), are used to mimic “follow the silverback” or “competition for adult females” behavior, respectively. Equation (8) is used if $C \geq W$, while (9) will be used if $C < W$, with W is set at the beginning of the optimization process.

$$GY(j+1) = C\cdot l\cdot \left|\frac{1}{NP}\sum_{i=1}^{NP} GY_i(j)\right|\cdot (Y(j) - Y_{\mathrm{sb}}) + Y(j) \quad (8)$$

$$GY(j+1) = Y_{\mathrm{sb}} - \beta\cdot D\cdot (2r_6 - 1)\big(Y_{\mathrm{sb}} - Y(j)\big) \quad (9)$$

where NP represents the population size of the gorillas and $GY_i(j)$ is the position vector of i-th gorilla at j-th iteration. r_6 is a value chosen randomly between 0 and 1 and β is assigned at the beginning of the optimization process. In (9), D is utilized to emulate the effect of violence on the dimensions of solutions. A random value r_7, generated between 0 and 1, determines the behavior of D. If $r_7 \geq 0.5$, D is assigned with a randomly selected value from a normal distribution (N_1). Otherwise, if $r_7 < 0.5$, D is assigned values randomly from the normal distribution and the dimensions of the problem (N_2).

$$D = \begin{cases} N_1 & r_7 \geq 0.5 \\ N_2 & r_7 < 0.5 \end{cases} \quad (10)$$

Figure 3 shows the pseudo code of the AGTO algorithm. As shown in the pseudo code, the algorithm starts with setting parameters such as β, W, p, NP, $j_{\max}$, Y_{LB} and Y_{UB}, along with initializing the gorilla population position.

4 Results and discussion

In this work, the performance of the AGTO-SHMPWM technique is evaluated through MATLAB analysis and compared with that of GA- and GOA-SHMPWM techniques. Table 2 shows the parameters of GA, GOA and AGTO algorithms. For a fair comparison, all three SC methods are initialized with the same number of runs, maximum number of iterations ($j_{\max}$) and population size (NP), which are set as 20, 500 and 100, respectively. Note that all these three SC methods are used to minimize the OF in (5) for a wide range of M_{idx}, which varies from 0.01 to 1.00 with a step size of 0.01.

Figure 4 compares the OF values achieved by the GA-, GOA- and AGTO-SHMPWM techniques. As can be seen in the figure, all SC methods produce similar OF values at M_{idx} near 0 and 1. However, in the regions between M_{idx} = 0.45 to 0.72 and 0.75 to 0.84, the OF values achieved by the AGTO are consistently below 10^{-30}, with a minimum of 10^{-32} significantly lower than the OF values of GA and GOA methods, which are higher than 10^{-12} in the same region. This suggests that the AGTO method exhibits an attractive behavior compared to other methods, potentially reflecting its capability to explore the solution space more thoroughly in these regions. Figure 5 shows the plot of the cumulative distribution function (CDF) versus OF plot for the GA, GOA and AGTO methods. The CDF is calculated using the following formula

$$CDF = P\big(OF \leq OF_{\mathrm{spec}}\big) \quad (11)$$

The CDF demonstrates the probability (P) that the OF is equal to or lower than a specific OF value (OF_{spec}). By way of example, for an OF_{spec} of 10^{-30} (refer to Fig. 5), the CDF of the AGTO method is 38%, while that of the GA and GOA methods are both 0%. This indicates that 38% of the *OF* values achieved by the AGTO method are below 10^{-30}, whereas the GA and GOA methods do not achieve any values below this threshold. Similarly, for an OF_{spec} of 10^{-12}, the *CDF* of the AGTO method is 38%, while that of the GA and GOA methods are both 0%. This shows that none of the *OF* values achieved by the GA and GOA methods are lower than 10^{-12}. The *CDF* results confirm that the AGTO method has a higher probability of achieving lower *OF* values compared to the GA and GOA methods.

```
Algorithm Pseudo code of AGTO algorithm
Start
Initialize parameters: β, W, p, NP, j_max, Y_LB and Y_UB
Initialize the population of gorilla (Y_1, Y_2, …, Y_NP)
Evaluate OF value of each gorilla
while (j < j_max)
Recalculate C using (7)
for each gorilla
Update position of gorilla using (6)
end for
Evaluate OF value of each gorilla
If GY's OF is better than Y's OF, replace Y with GY; else, keep Y
Best position of gorilla is chosen as Y_sb
for each gorilla
    if (|C| ≥ W)
    Update position of gorilla using (8)
    else
    Update position of gorilla using (9)
    end if
end for
Evaluate the OF value of each gorilla
Replace Y_sb if there is a better solution
j = j + 1
end while
Final Y_sb is chosen as the optimal solution.
End
```

Fig. 3. Pseudo code of AGTO algorithm

Table 2. Parameters of soft-computing methods employed in MATLAB analysis

Algorithms	GA	GOA	AGTO
Parameters	Crossover = 0.5 Mutation = 0.5	$Y_{LB} = 0°$ $Y_{UB} = 90°$ $f = 0.50$ $l = 1.50$ $c_{min} = 0.00004$ $c_{max} = 1.00$	$Y_{LB} = 0°$ $Y_{UB} = 90°$ $\beta = 3.00$ $p = 0.03$ $W = 0.80$

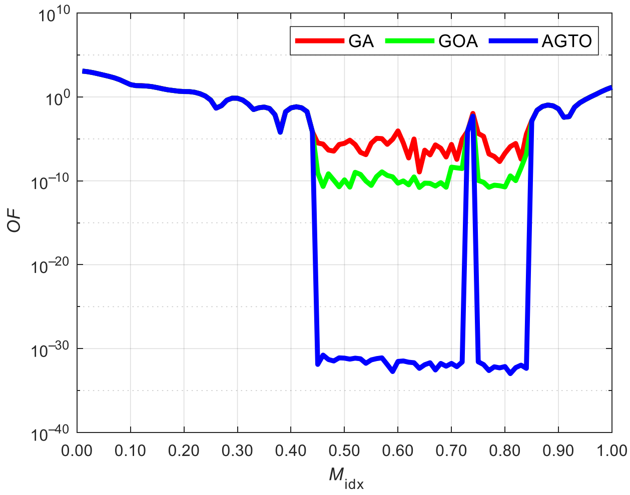

Fig. 4. *OF* obtained using GA-, GOA- and AGTO-SHMPWM techniques

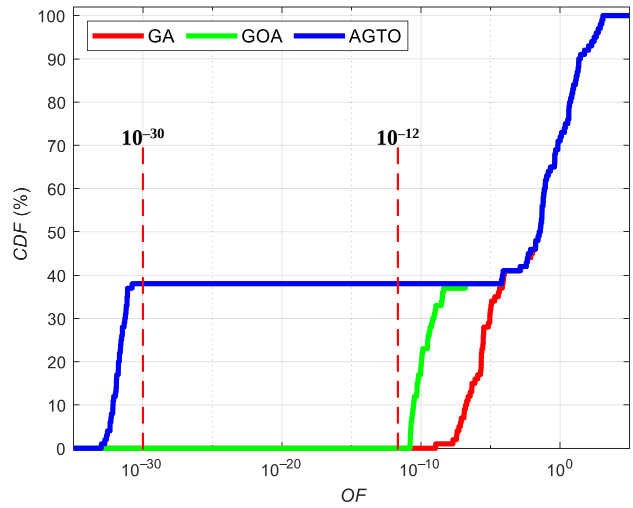

Fig. 5. *CDF* obtained using GA-, GOA- and AGTO-SHMPWM techniques

Figure 6 shows the switching angles obtained using AGTO-SHMPWM technique for M_{idx} ranging from 0.01 to 1.00. Clearly, the figure shows that the AGTO-SHMPWM technique can provide switching-angle solutions over a wide range of M_{idx}. Besides, the condition of $0 \leq \alpha_1 \leq \alpha_2 \leq \alpha_3 \leq \alpha_4 \leq \alpha_5 \leq \pi/2$ is met. Additionally, the switching angles tend to decrease from 90° to 0° in order to increase the amplitude of the fundamental output voltage harmonic (V_1). The switching angles computed from the proposed AGTO-SHMPWM technique are substituted into (2) to calculate V_1, V_3, V_5, V_7, V_9, V_{11}, V_{13} and V_{15}, which help assess the performance of the AGTO-SHMPWM technique. Figure 7 illustrates the harmonic response achieved by the AGTO-SHMPWM technique. As depicted in the figure, the fundamental harmonic (V_1) closely matches the desired value (100%) over the M_{idx} range. From M_{idx} = 0.43 to M_{idx} = 0.85, it can be noticed that the undesired harmonics (V_5, V_7, V_{11} and V_{13}) are nearly zero, reflecting the successful minimization of *OF* achieved by the proposed AGTO-SHMPWM technique. Thus, Fig. 7 clearly shows that the proposed AGTO-SHMPWM technique can maintain the fundamental voltage of the MLI over a wide range of M_{idx}, while minimizing the undesired low-order harmonics. Figure 8 compares the phase and line-to-line voltage THDs produced by the AGTO-SHMPWM technique. Clearly, the line-to-line voltage THDs are always lower compared to the THDs of the phase voltage. This is attributed to the natural elimination of triplen-odd harmonics in the 3-ph system, as mentioned earlier. As shown in Fig. 8, the proposed AGTO-SHMPWM technique achieves a minimum phase voltage THD of 7.93% at M_{idx} = 0.80. At this M_{idx}, the corresponding line-to-line THD is 5.55%.

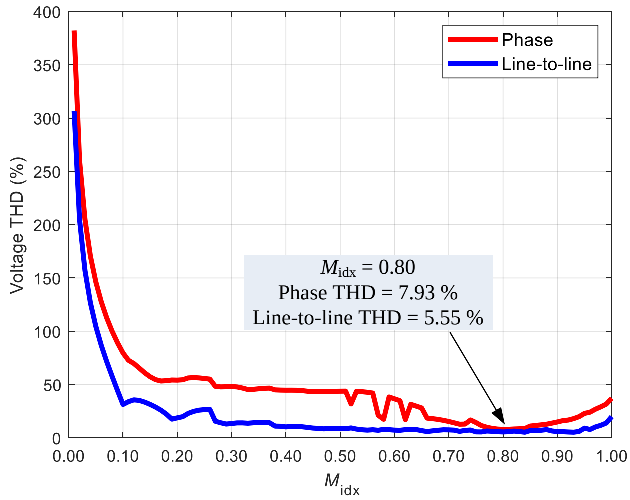

Fig. 8. THDs of phase and line-to-line voltage waveforms over M_{idx} range determined using AGTO-SHMPWM techniques

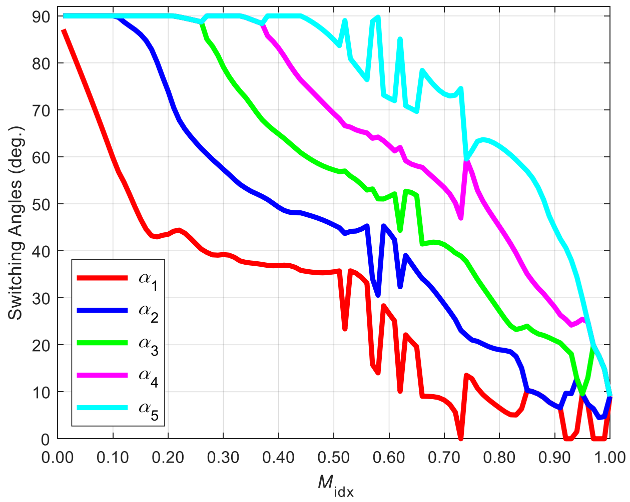

Fig. 6. Switching angles over M_{idx} range determined using AGTO-SHMPWM techniques

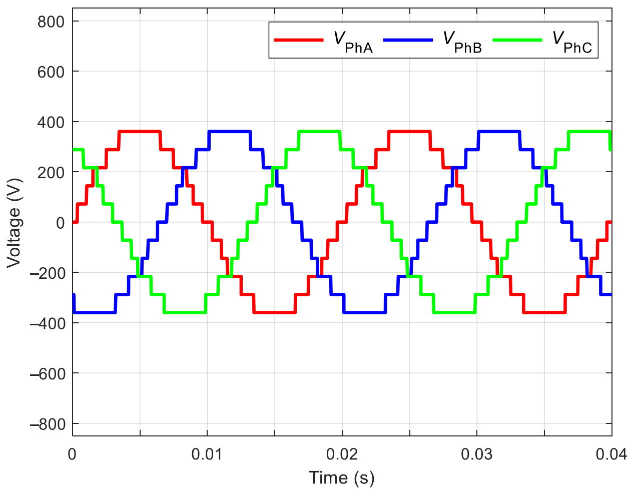

Fig. 9. Phase voltage waveforms (M_{idx} = 0.80)

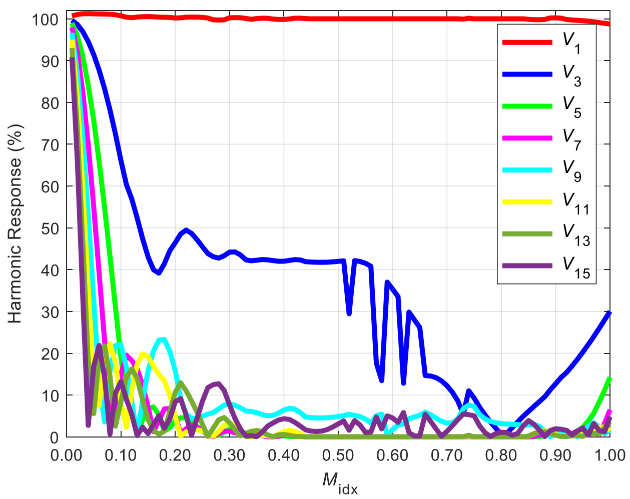

Fig. 7. Harmonic response over M_{idx} range determined using AGTO-SHMPWM techniques

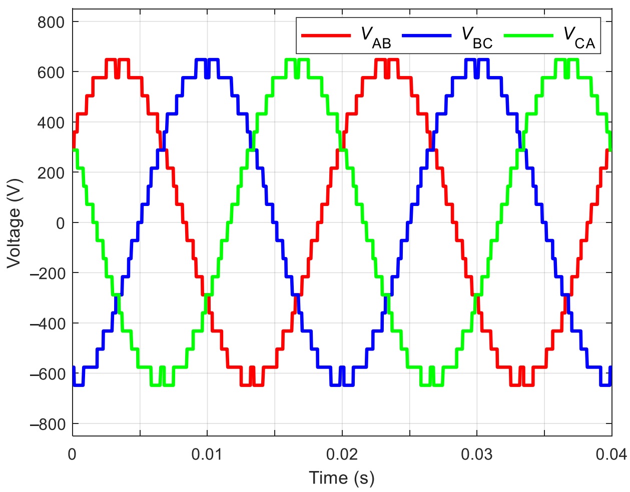

Fig. 10. Line-to-line voltage waveforms (M_{idx} = 0.80)

The switching angles computed using the AGTO-SHMPWM technique are applied to a 3-ph 11L S2MLI PSIM simulation model, constructed based on the configuration shown in Fig. 1, for further validation. The S2MLI is controlled to operate at a fundamental frequency of 50 Hz. A set of switching angles, obtained from the AGTO-SHMPWM technique at M_{idx} = 0.80, is applied to the 3-ph 11L S2MLI model. Note that the switching angles applied to phase B are shifted by 120°, while those of phase C are shifted by 240°. Each DC voltage source in the model is set to 72 V, and the S2MLI is tested under both resistive and inductive loads. For a fair comparison, the total load impedance is kept constant at 62.43 Ω for both load conditions. The resistive load is set to R = 62.43 Ω, while the inductive load consists of R = 50 Ω and L = 119 mH. Figure 9 shows the output phase voltage waveform of the 3-ph 11L S2MLI operated under both resistive and inductive loads, while that of line-to-line voltage waveform is shown in Fig. 10. Note that the phase and line-to-line voltage waveforms are identical under both resistive and inductive loads. Hence, the output voltage waveforms are presented only once in Figs. 9 and 10. As shown in the figures, the voltage waveforms generated using the switching angles calculated from the AGTO-SHMPWM technique are sinusoidal-like staircase shape, with each waveform having a phase shift of 120° from its adjacent phase. Besides, the voltage amplitude of the phase voltage waveform is 360.00 V, while that of the line-to-line voltage waveform is 648.00 V.

Figures 11(a) and 11(b) compare the waveforms of phase A voltage (V_{PhA}), line-to-line AB voltage (V_{AB}) and line A current (I_{LineA}) of 3-ph 11L S2MLI when operated with resistive and inductive loads, respectively. The harmonic spectrums of the voltage (V_{PhA} and V_{AB}) are shown in Fig. 12, while the harmonic spectrums of the current (I_{LineA} under resistive load and I_{LineA} under inductive load) are compared in Fig. 13. All harmonic spectrums are obtained using the Fast Fourier Transform (FFT) analysis in PSIM software.

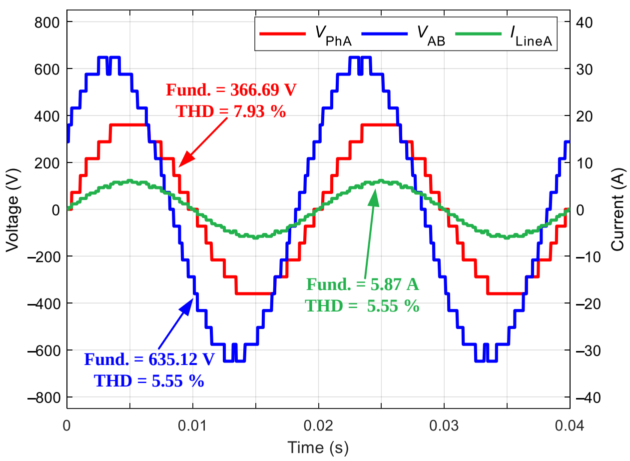

(a)

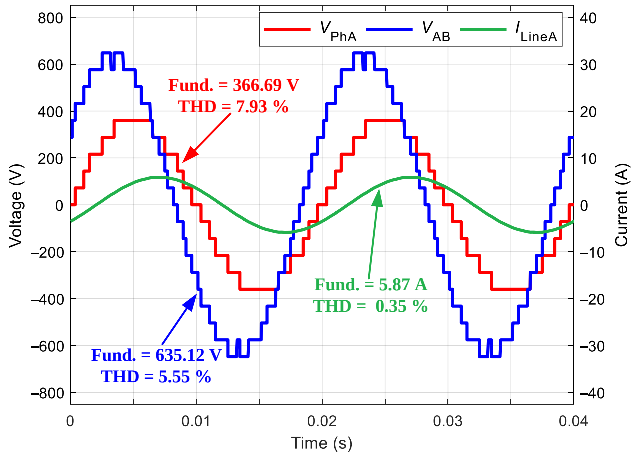

(b)

Fig. 11. Comparison of V_{PhA}, V_{AB} and I_{LineA} waveforms (M_{idx} = 0.80): (a) Resistive load, (b) Inductive load

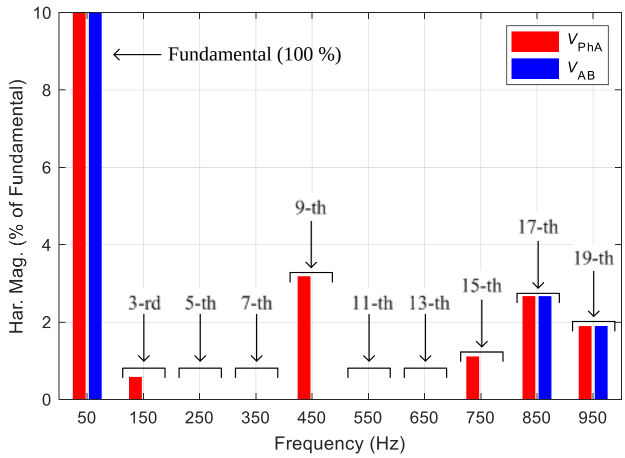

Fig. 12. Harmonics spectrums of V_{PhA} and V_{AB} waveforms (M_{idx} = 0.80)

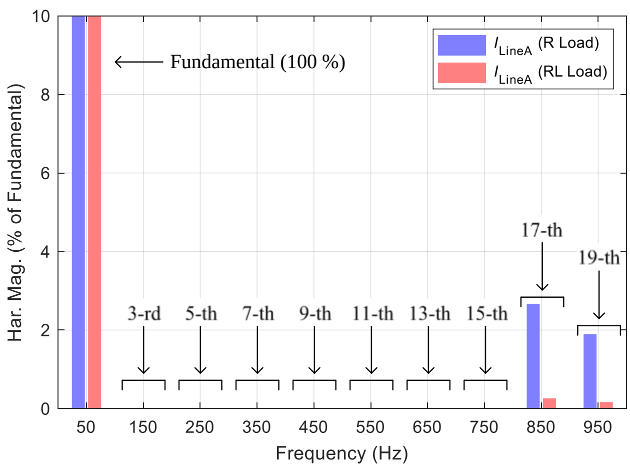

Fig. 13. Harmonics spectrums of I_{LineA} waveforms under resistive and inductive loads (M_{idx} = 0.80)

Note that due to the wye-connection in the 3-phase system, the load phase current is the same as the line current, therefore, only the line current results are presented. As can be seen in Figs. 11(a) and 11(b), V_{AB} leads V_{PhA}, reflecting the phase shift between the line-to-line and phase voltages in a 3-ph system, which is aligned with the 3-ph circuit theory [26]. Additionally, as shown Fig. 11(a), the I_{LineA} is in phase with V_{PhA}, which is due to the resistive nature of the load, while I_{LineA} lag V_{PhA}, as shown in Fig. 11(b), which is attributed to the inductive nature of the load. The fundamental components of V_{PhA} and V_{AB} are 366.69 V and 635.12 V, respectively, while the fundamental component of I_{LineA} is 5.87 A. Note that the fundamental voltage of V_{PhA} obtained from the FFT analysis closely matches the calculation from (3), while that of V_{AB} is √3 times the fundamental voltage of V_{PhA}. The THD of V_{AB} is 5.55%, lower than the THD of V_{PhA}, which is 7.93%. This reduction in THD in V_{AB} results from the natural elimination of triplen-odd harmonics (e.g., V_3, V_9 and V_{15}) in V_{AB}, as evidenced in Fig. 12. Besides, as can be seen in Fig. 12, the V_5, V_7, V_{11} and V_{13} harmonics of the phase voltage waveform are zero, which are the same as the harmonic responses observed at M_{idx} = 0.80 in Fig. 7. As shown in Figs. 11(a) and 11(b), the THDs of I_{LineA} under resistive and inductive loads are 5.55% and 0.35%, respectively. The I_{LineA} waveform for the inductive load is smoother and closer to a sinusoidal shape, leading to a significantly lower THD compared to that of resistive load. The lower I_{LineA} THD is primarily attributed to the inductive load, which acts like a low-pass filter that inherently attenuates higher-order harmonics. Additionally, since the line-to-line voltage does not contain triplen-odd harmonics, these harmonics are also absent in the I_{LineA} waveform, as shown in Fig. 13. Apart from the harmonic analysis, the performance of the 3-ph 11L S2MLI controlled at M_{idx} = 0.80 using the switching angles obtained using AGTO-SHMPWM technique has been evaluated under changing frequency conditions. Figure 14 presents the V_{PhA} and V_{AB} waveforms when frequency changes from 50 Hz to 100 Hz at 0.08 s and back to 50 Hz at 0.12 s. As can be observed from the figure, the output voltage waveforms are able to respond instantly to the frequency step-change without any deterioration. This demonstrates that the MLI, controlled using the switching angles obtained from AGTO-SHMPWM technique, can maintain a stable output voltage waveform despite frequency changes.

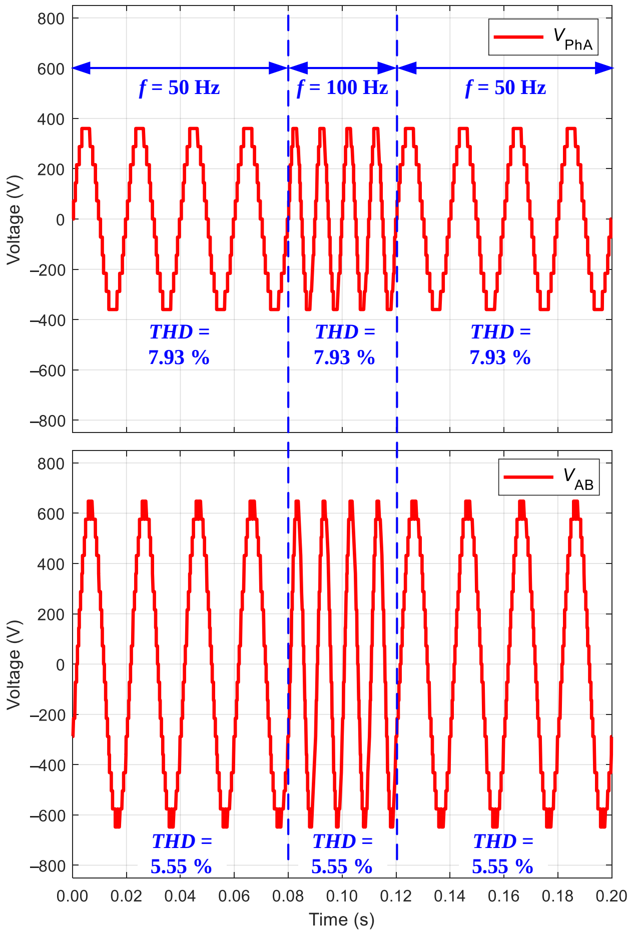

Fig. 14. Voltage waveforms with changing frequency (M_{idx} = 0.80)

5 Conclusion

In this paper, AGTO-SHMPWM technique is proposed to determine the switching angles for 3-ph 11L S2MLI. The performance of the AGTO-SHMPWM technique has been compared to that of GA and GOA-SHMPWM techniques. MATLAB analysis results show that proposed AGTO-SHMPWM technique can achieve significantly lower *OF* values, below 10^{-30}, compared to GA- and GOA-SHMPWM techniques (higher than 10^{-12}). The *CDF* analysis reveals that the AGTO method has a 38% probability of achieving an *OF* lower than 10^{-30}, while the GA and GOA methods have a 0% probability. This demonstrates that the AGTO method has a higher probability of achieving lower *OF* values compared to the GA and GOA methods. The switching angles obtained using the AGTO-SHMPWM technique are able to minimize the undesired harmonics (V_5, V_7, V_{11} and V_{13}) while maintaining the desired fundamental harmonic.

In addition, PSIM simulation results demonstrate that the switching angles obtained using the AGTO-SHMPWM technique, when applied to the 3-ph 11L S2MLI operated under pure resistive and inductive loads, produce sinusoidal-like staircase output voltage wave-forms. The phase and line-to-line voltage THDs, when the S2MLI is operated at M_{idx} of 0.80, are 7.93% and 5.55%, respectively, which are consistent with those predicted by MATLAB analysis. Besides, the 3-ph 11L S2MLI, controlled using the switching angles obtained from AGTO-SHMPWM technique, can maintain a stable output voltage waveform despite frequency changes.

Acknowledgement

This work was supported by the Ministry of Higher Education Malaysia through the Fundamental Research Grant Scheme (FRGS/1/2022/TK08/UNIMAP/02/63).

References

[1] A. Poorfakhraei, M. Narimani and A. Emadi, “A Review of Multilevel Inverter Topologies in Electric Vehicles: Current Status and Future Trends”, *IEEE Open Journal of Power Electronics*, vol. 2, pp. 155-170, Mar. 2021. doi: 10.1109/OJPEL.2021.3063550

[2] M. F. M. Elias, N. A. Rahim and N. F. Rosli, “A Three-phase Hybrid Multilevel Inverter with Enhanced Pulse-width Modulation Strategy”, *IEEE Transactions on Power Electronics*, vol. 38, no. 4, pp. 4714-4726, Apr. 2023. doi: 10.1109/TPEL.2022.3228546

[3] A. Taiea, E. E. M. Mohamed, A. Youssef, A. A. Ibrahim, M. S. R. Saeed and A. I. M. Ali, “Three Phase Modular Multilevel Inverter-based Multi-terminal Asymmetrical DC Inputs for Renewable Energy Applications”, *Engineering Science and Technology, An International Journal*, vol. 23, no. 4, pp. 831-839, 2020. doi: 10.1016/j.jestch.2019.11.003

[4] V. F. Pires, D. Foito and J. F. Silva, “Fault-tolerant Multilevel Topology Based on Three-phase H-bridge Inverters for Open-end Winding Induction Motor Drives”, *IEEE Transactions on Energy Conversion*, vol. 32, no. 3, pp. 895-902, Sep. 2017. doi: 10.1109/TEC.2017.2693563

[5] B. Sirisha and P. S. Kumar, “Modified Diode Clamped Inverter Fed AC Motor Drives for Traction Applications”, in *2024 International Conference on Electrical Engineering and Computer Science (ICECOS)*, Palembang, Indonesia, 2019. doi: 10.1109/ICECOS63900.2024.10791137

[6] M. Kim, J. Pribadi and D. Lee, “A Novel Three-phase Seven-level Hybrid Flying-capacitor Inverter”, in *2022 IEEE Energy Conversion Congress and Exposition (ECCE)*, Detroit, MI, USA, 2022. doi: 10.1109/ECCE50734.2022.9947405

[7] N. Janjamraj and A. Oonsivilai, “Harmonic Elimination of Hybrid Multilevel Inverters Using Particle Swarm Optimization”, *International Journal of Electrical and Computer Engineering*, vol. 5, no. 12, pp. 1461-1466, Dec. 2012. doi: 10.5281/zenodo.1333090.svg

[8] M. H. Yabalar and E. Ercelebi, “Hybrid Optimization Based Harmonic Minimization in Three Phase Multilevel Inverter with Reduced Switch Topology”, *IEEE Access*, vol. 12, no. 4, pp. 71010-71023, May 2024. doi: 10.1109/ACCESS.2024.3401730

[9] J. A. Juárez-Abad, J. L. Barahona-Avalos and J. Linares-Flores, “PWM Techniques for an Asymmetric Multilevel Binary Inverter: An FPGA-based Implementation”, *IET Power Electronics*, vol. 14, no. 8, pp. 1529-1539, May 2021. doi: 10.1049/pel2.12131

[10] E. Can and H. H. Sayan, “Development of Fractional Sinus Pulse Width Modulation with β Gap on Three Step Signal Processing”, *International Journal of Electronics*, vol. 110, no. 3, pp. 527-546, Feb. 2022. doi: 10.1080/00207217.2022.2040056

[11] O. Dordevic, M. Jones and E. Levi, “A Comparison of Carrier-based and Space Vector PWM Techniques for Three-level Five-phase Voltage Source Inverters”, *IEEE Transactions on Industrial Informatics*, vol. 9, no. 2, pp. 609-619, May 2013. doi: 10.1109/TII.2012.2220553

[12] A. Hiendro, I. Yusuf, J. Junaidi, T. P. Wigyarianto and Y. M. Simanjuntak, “Optimization of SHEPWM Cascaded Multi-level Inverter Switching Patterns”, *International Journal of Power Electronics and Drive Systems*, vol. 11, no. 3, pp. 1570-1578, Sep. 2020. doi: 10.11591/ijpeds.v11.i3.pp1570-1578

[13] M. S. A. Dahidah and V. G. Agelidis, “Selective Harmonic Elimination PWM Control for Cascaded Multilevel Voltage Source Converters: A Generalized Formula”, *IEEE Transactions on Power Electronics*, vol. 23, no. 4, pp. 1620-1630, Jul. 2008. doi: 10.1109/TPEL.2008.925179

[14] Krismadinata, N. A. Rahim, H. W. Ping and J. Selvaraj, “Elimination of Harmonics in Photovoltaic Seven-level Inverter with Newton-Raphson Optimization”, *Procedia Environmental Sciences*, vol. 17, pp. 519-528, 2013. doi: 10.1016/j.proenv.2013.02.067

[15] S. Padmanaban, C. Dhanamjayulu and B. Khan, “Artificial Neural Network and Newton Raphson (ANN-NR) Algorithm Based Selective Harmonic Elimination in Cascaded Multilevel Inverter for PV Applications”, *IEEE Access*, vol. 9, pp. 75058-75070, May 2021. doi: 10.1109/ACCESS.2021.3081460

[16] S. Ahmad, M. Meraj, A. Iqbal and I. Ashraf, “Selective Harmonics Elimination in Multilevel Inverter by a Derivative-free Iterative Method under Varying Voltage Condition”, *ISA Transactions*, vol. 92, pp. 241-256, 2019. doi: 10.1016/j.isatra.2019.02.015

[17] A. M. Amjad and Z. Salam, “A Review of Soft Computing Methods for Harmonics Elimination PWM for Inverters in Renewable Energy Conversion Systems”, *Renewable and Sustainable Energy Reviews*, vol. 33, pp. 141-153, 2014. doi: 10.1016/j.rser.2014.01.080

[18] D. G. Kumar, N. V. Sireesha, N. Bhoopal, R. K. Gatla, H. Kotb, K. M. AboRas, A. Elrashidi, M. Alqarni, Y. Y. Ghadi and A. Oubelaid, “Application of Soft Computing Algorithms for Hybrid Modular Multilevel Inverters”, *Measurement: Sensors*, vol. 31, no. 100999, pp. 1-16, Dec. 2023. doi: 10.1016/j.measen.2023.100999

[19] M. Steczek, W. Jefimowski and A. Szeląg, “Application of Grasshopper Optimization Algorithm for Selective Harmonics Elimination in Low-frequency Voltage Source Inverter”, *Energies*, vol. 13, no. 23, pp. 1-16, Dec. 2020. doi: 10.3390/en13236426

[20] M. P. Perumal and D. Nanjudapan, “Performance Enhancement of Embedded System Based Multilevel Inverter Genetic Algorithm”, *Journal of Electrical Engineering*, vol. 62, no. 4, pp. 190-198, 2011. doi: 10.2478/v10187-011-0031-1

[21] B. Abdollahzadeh, F. S. Gharehchopogh and S. Mirjalili, “Artificial Gorilla Troops Optimizer: A New Nature-inspired Metaheuristic Algorithm for Global Optimization Problems”, *International Journal of Intelligent Systems*, vol. 36, no. 10, pp. 1-72, Jul. 2021. doi: 10.1002/int.22535

[22] M. A. El-Dabah, M. H. Hassan, S. Kamel and H. M. Zawbaa, "Robust Parameters Tuning of Different Power System Stabilizers Using a Quantum Artificial Gorilla Troops Optimizer", *IEEE Access*, vol. 10, pp. 82560-82579, 2022. doi: 10.1109/ACCESS.2022.3195892

[23] A. Fathy and D. Yousri, "An Efficient Artificial Gorilla Troops Optimizer-based Tracker for Harvesting Maximum Power from Thermoelectric Generation System", *Applied Thermal Engineering*, vol. 234, no. 121290, pp. 1-17, Aug. 2023. doi: 10.1016/j.applthermaleng.2023.121290

[24] E. H. Houssein, M. R. Saad, A. A. Ali and H. Shaban, "An Efficient Multi-objective Gorilla Troops Optimizer for Minimizing Energy Consumption of Large-Scale Wireless Sensor Networks", *Expert Systems with Applications*, vol. 212, no. 118827, pp. 1-23, 2023. doi: 10.1016/j.eswa.2022.118827

[25] N. Farokhnia, S. H. Fathi, R. Salehi, G. B. Gharehpetian and M. Ehsani, "Improved Selective Harmonic Elimination Pulse-width Modulation Strategy in Multilevel Inverters", *IET Power Electronics*, vol. 5, no. 9, pp. 1904-1911, Nov. 2012. doi: 10.1049/iet-pel.2011.0293

[26] M. N. O. Sadiku, *Fundamentals of Electric Circuits*, 7th ed. New York: McGraw-Hill Education, 2020.

Received 6 January 2025